

PAPER

Thermal shrinkage and stability of diamondene nanotubes

To cite this article: Lei Wang *et al* 2019 *Nanotechnology* **30** 075702

View the [article online](#) for updates and enhancements.



IOP | ebooks™

Bringing you innovative digital publishing with leading voices to create your essential collection of books in STEM research.

Start exploring the [collection](#) - download the first chapter of every title for free.

Thermal shrinkage and stability of diamondene nanotubes

Lei Wang¹ , Kun Cai², Yi Min Xie²  and Qing-Hua Qin³ 

¹ Department of Engineering Mechanics, College of Mechanics and Materials, Hohai University, Nanjing 211100, People's Republic of China

² Centre for Innovative Structures and Materials, School of Engineering, RMIT University, Melbourne 3001, Australia

³ School of Engineering, Australian National University, Canberra 2600, Australia

E-mail: kun.cai@rmit.edu.au

Received 2 September 2018, revised 7 November 2018

Accepted for publication 26 November 2018

Published 18 December 2018



CrossMark

Abstract

By curving a rectangular diamondene, an sp^2/sp^3 composite carbon film, a diamondene nanotube (DNT) can be formed when the two straight edges are sewn together. In this study, thermal stabilities of DNTs are investigated using molecular dynamics simulation approaches. An interesting thermal shrinkage of damaged DNTs is discovered. Results indicate that DNTs have critical temperatures between 320 K and 350 K. At temperatures higher than the critical value, the interlayer bonds, i.e., the sp^3-sp^3 bonds, may break. The broken ratio of the interlayer bonds mainly depends on the temperature. For the DNT with a high broken ratio of interlayer bonds, it has thermal shrinkage in both the cross section and tube axis. The sp^2-sp^3 bonds in either the inner or the outer surface are much more stable. Even at 900 K, only a few sp^2-sp^3 bonds break. These properties can be used in the design of metamaterials.

Keywords: diamondene, nanotube, thermal shrinkage, thermal stability, molecular dynamics

(Some figures may appear in colour only in the online journal)

1. Introduction

Due to particular ground-state electron configuration of $1s^2 2s^2 2p^2$, carbon has many allotropes. Fullerene [1], carbon nanotube (CNT) [2–4], and graphene [5–7] belong to the sp^2 carbon materials with different dimensions, while diamond and lonsdaleite [8] can be considered as the sp^3 carbon materials. For the sp^2 materials, e.g., CNT or graphene, they have excellent electrical conductivity because each carbon atom has a delocalized electron. However, the sp^3 materials behave as insulators since all the electrons of each carbon atom are used to form covalent bonds. For the same reason, the optical properties of the allotropes are also different. In some nano-devices, e.g., nano-oscillators [9–12] and nanomotors [13–16], multi-physical properties are often required simultaneously. Hence, it is desirable to develop new kinds of carbon material to meet various requirements.

Among artificial carbon materials, two-dimensional diamond film has attracted much attention in recent years [17–26] and its composite sp^2/sp^3 electron configuration was

discovered years ago [17]. Chernozatonskii *et al* [18, 19] studied the mechanical and electrical properties of new two-dimensional materials (C_xH layer, hydrogenated diamond films). Recently, Martins *et al* [24] reported the fabrication and characterization of two or several layers of graphene, which is called diamondene with a composite sp^2/sp^3 electron configuration, through phase transition under extremely high pressure, e.g., over 10 GPa. Gao *et al* [25] evaluated the mechanical properties of diamondene attached to an SiC (0001) substrate. They found that diamondene has a reversible drop in electrical conductivity upon indentation and the band gap is ~ 2 eV when estimated by density functional theory-based calculation. Shi *et al* [26] used molecular dynamics simulations to estimate the thermal stability, tensile stiffness, and strength of diamondene. Results show that the interlayer bonds, i.e., the sp^3-sp^3 bonds, in diamondene may break without any external pressure at room temperature (300 K). Besides, the stiffness and strength of diamondene depend on loading direction.

Inspired by the idea of forming a CNT from curved graphene, Cai *et al* [27] built diamondene nanotubes (DNTs) from curved diamondene ribbon. Due to different bond topology, DNTs have higher buckling stability under compression or torsion than the double-walled CNTs with similar diameter. Recently, Wang *et al* [28] discovered that DNTs have softening-to-hardening behavior under uni-axial tension. The mechanism was explored. The DNT tube behaves as softening because the sp^2 - sp^3 bonds in the outer layer experience a transition from pre-stretched state to shrinking firstly. However, with the increase of the axial strain, the bonds in the outer layer begin to resist the axial deformation and hardening behavior thus appears.

For a nanosystem working at a finite temperature, its thermal stability is essential to its function. In this study, we focus on the thermal stability of DNTs. The effects of temperature, diameter, and length of tubes on its thermal stability are investigated through simulations on numerous models of DNTs.

2. Models and methodology

2.1. Models of DNTs

In figure 1(a), the geometry of a diamondene ribbon is shown. As an sp^2/sp^3 composite lattice structure, it has two types of carbon atoms, i.e., the sp^2 atoms (in black or yellow) and the sp^3 atoms (in blue or pink). When curved along the armchair direction, the ribbon with periodic boundaries can form an armchair DNT (A-DNT), e.g., figure 1(b), if the atoms in the two straight edges are covalently bonded, correspondingly. Here, we label the DNT with chiral index ((m , m)). In the same way, one can obtain a zigzag DNT (Z-DNT) by curving the ribbon along the zigzag direction. We label the DNT with chiral index ((n , 0)).

To describe deformation of the DNT, eight representative atoms (upper right in figure 1(a)) are chosen. Four of them are in the inner layer and the rest are in the outer layer of the DNT. The mean diameters of the two layers, i.e., d_I and d_O (figure 1(b)), can be estimated via the representative bond lengths and bond angles. According to the types of the neighboring covalently bonded atoms, the bonds can be classified into two types. One is the sp^2 - sp^3 bond, e.g., bonds 1-3, 0-2, 5-3, 4-2, 5-7, and 4-6, while the other is the sp^3 - sp^3 bond, e.g., bonds 2-3 and 6-7. The bond length of a bond, e.g., 1-3, is labeled as L13. Bond angles are also essential to estimate the diameters. The bond angle between two neighboring bonds, e.g., bonds 1-3 and 3-5, is labeled as α_{135} in which the middle digit in subscript is the corner of the angle.

The mean diameters of the two layers in an A-DNT can be obtained by calculating the following formula:

$$d_I = \sim 2m \times [L02 + L24 \times (-\cos \alpha_{024})] / \pi; \quad (1a)$$

$$d_O = \sim 2m \times [L13 + L35 \times (-\cos \alpha_{135})] / \pi. \quad (1b)$$

The formula for estimating the mean diameters of the two layers in a Z-DNT reads as

$$d_I = \sim n \times [(L24 + L46) \times \sin(\alpha_{246}/2)] / \pi; \quad (2a)$$

$$d_O = \sim n \times [(L35 + L57) \times \sin(\alpha_{357}/2)] / \pi. \quad (2b)$$

2.2. Methodology

Here, molecular dynamics simulations are adopted to investigate the thermal stability of DNTs. The simulations are performed using the open source code LAMMPS [29]. Each simulation contains six main steps. Firstly, a DNT model is built by a geometrical mapping method [30] from two layers of graphene with the AA stacking. Secondly, the DNT is in a simulation box with SSP boundary conditions in the x -/ y -/ z -directions, respectively. Here, 'S' means non-periodic and shrink-wrapped boundary, and 'P' means periodic boundary. The size of the box in the z -direction is accurately set to keep the two edges of the tube bonded covalently. Thirdly, the tube is reshaped by minimizing the potential energy of the system. Fourthly, the atoms in the DNT are assigned with initial velocities which satisfies the Gaussian distribution. Fifthly, the system is put in an NPT (constant atom number, pressure and temperature) ensemble with null pressure along the z -direction. A Nosé-Hoover thermostat [31, 32] is used to control the temperature. Finally, the important data are recorded for post-processing.

In the present work, the interactions between neighboring atoms are evaluated by the adaptive intermolecular reactive empirical bond order (AIREBO) potential [33], which has been widely used in the simulation of hydrocarbon systems [14, 24, 34, 35]. During the time integration, the increment of time is set to 0.001 ps in each step. Each simulation contains 500 000 time steps.

3. Results and discussion

3.1. Thermal stability of DNTs at finite temperatures

To demonstrate the dependency of DNTs' stability on essential factors, i.e., curvature radius, chirality, and temperature, we choose 18 different A-DNTs and 18 different Z-DNTs in thermal relaxation at finite temperatures from 1 K-900 K. The tube with a higher chiral index has a bigger radius (or lower curvature). When put the DNTs in a thermostat, their potential energy changes dependently on the essential factors. Figure 2 shows the variation of potential energy (VPE) of some representative DNTs at a low temperature of 1 K and a high temperature of 900 K.

Figure 2 gives the histories of potential energy per atom during relaxation of the DNTs at 1 K and 900 K. The four figures support the same conclusion, i.e., the potential energy per atom is higher in the DNT with smaller radius. The differences among the curves are also clear. For example, at 1 K, the values of the VPE per atom drop monotonously with the increase of the radii of DNTs. Furthermore, the values of the VPE per atom are independent on the chirality of the DNTs with similar radii. For example, A-DNT ((18, 18)) and Z-DNT ((31, 0)) have similar radii, and their VPE values have a slight difference. At 1 K, the values of the VPE converge within a few picoseconds for both types of DNTs.

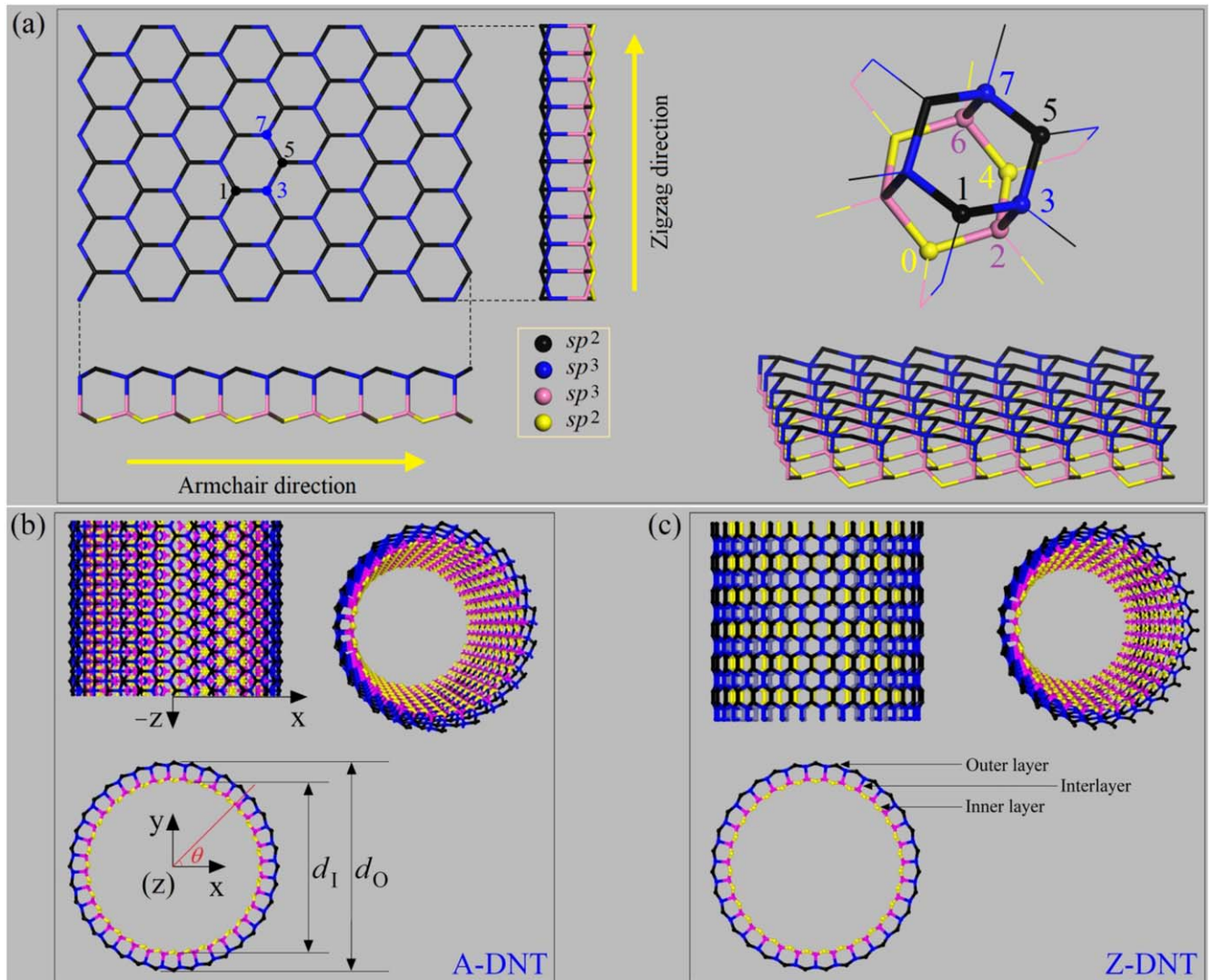


Figure 1. Schematic of configurations of diamondene and DNTs. (a) Diamondene ribbon and representative cell. (b) Armchair DNTs (A-DNTs) with a chiral index of $((m, m))$. (c) Zigzag DNTs (Z-DNTs) with a chiral index of $((n, 0))$. The axes of the tubes are aligned with the z -axis.

However, at 900 K, the values of the VPE per atom in the DNTs increase with tube radii. Moreover, the values of the VPE per atom at this temperature are one order of magnitude larger than those at 1 K. Such a high decrease of atom potential energy implies that the bond configurations in the tubes vary during relaxation. It can be partly illustrated by the longer duration for the convergence of the potential energy curves at 900 K.

To qualitatively estimate the difference in the DNTs after full relaxation, their states are listed in table 1. When a tube is stable, i.e., the number of broken bonds should be less than $m/6$ in an A-DNT $((m, m))$ or less than $n/12$ in a Z-DNT $((n, 0))$ after relaxation, the state of the tube is marked as 'S' and highlighted in blue. When the tube only has the interlayer sp^3-sp^3 bond breakage, it is marked as 'I' and highlighted in green. If the tube has serious deformation accompanied by bond breakage in both the inner and outer layers after relaxation, then the state is marked as 'NT' and highlighted in red.

Table 1 illustrates four characteristics of DNTs' states. Firstly, for a stable DNT at high temperature, it must be stable at lower temperatures, which does not depend on tube chirality. Secondly, at the same temperature no higher than 300 K, if a DNT with higher radius is unstable, the DNTs with lower radii must be unstable. Thirdly, a Z-DNT with smaller radius will be easily in an 'NT' state at temperature higher than 350 K. But for a slimmer A-DNT, it is in an 'NT' state only at 900 K or higher temperature. Finally, the interlayer bonds, i.e., the sp^3-sp^3 bonds, in the DNTs are not stable when the temperature is higher than 300 K, which is also independent of tube chirality. Actually, a free diamondene ribbon without passivation, which can be considered as a DNT with zero curvature, is unstable at room temperature due to the interlayer bond breaking [26].

3.2. Critical temperature for a stable DNT

The results in table 1 demonstrate that there must be a maximum temperature at which a DNT is in critical stable state.

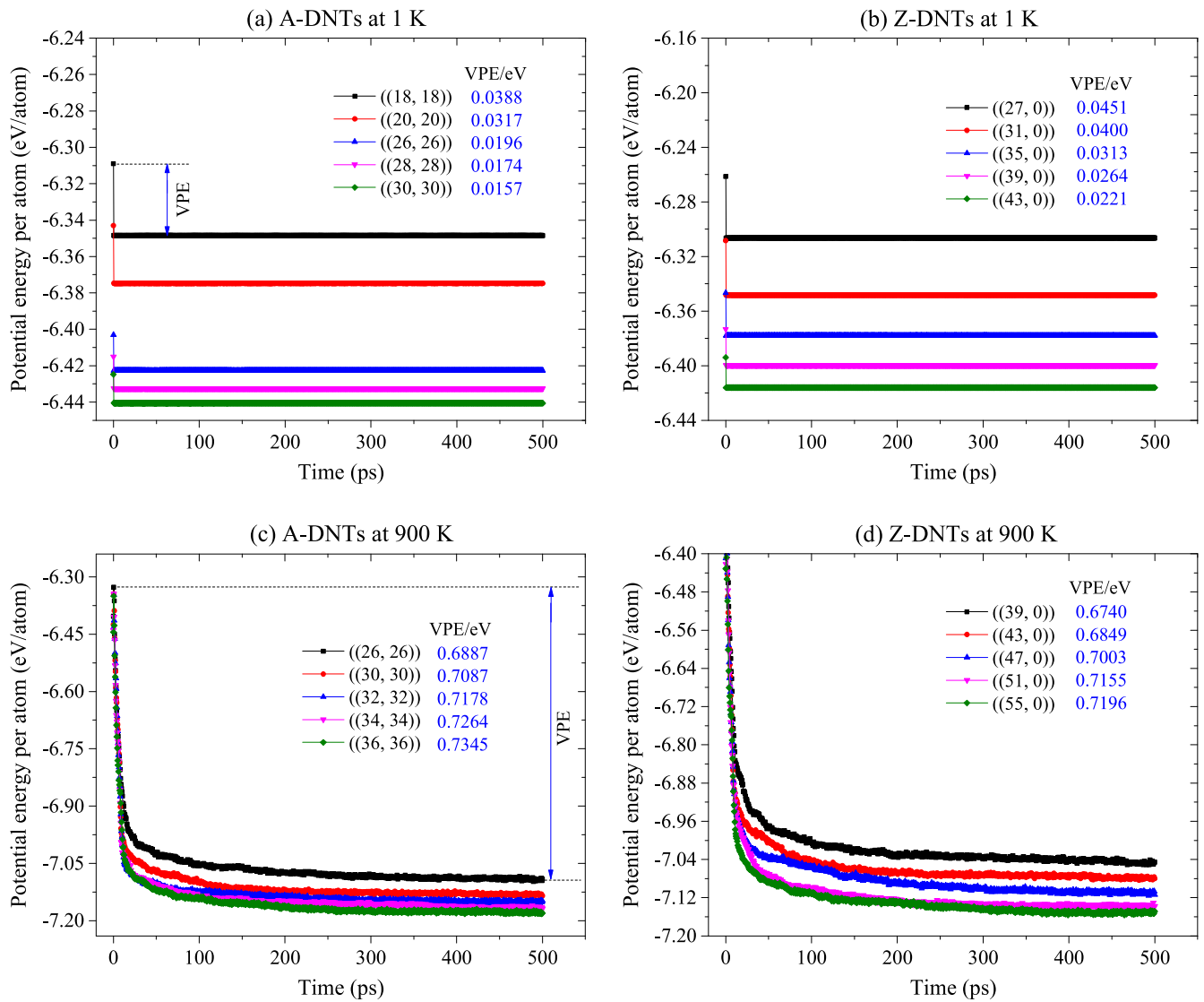


Figure 2. Histories of potential energy per atom of different DNTs during free relaxation at 1 K and 900 K.

At a temperature higher than the maximum, the tube will be in an unstable state, e.g., the number of broken bonds is higher than $m/6$ in an A-DNT $((m, m))$ or $n/12$ in a Z-DNT $((n, 0))$ after relaxation. Here, the maximum temperature is called the critical temperature for the DNT.

From table 1, the critical temperatures must be between 1 K and 350 K. To obtain the critical values, the bi-section algorithm [36] is adopted. For example, when the initial interval of the temperature is [10, 400] K, the value of the median is 205 K. If the tube is stable after relaxation at 205 K, then the interval is updated to be [205, 400] K. Otherwise, the new interval is [10, 205] K. When the width of the interval is less than 1 K, the median of the interval is the critical temperature of the tube. Considering the effect of the random distribution of the initial velocities of the atoms on the tube's stability, the integer part of each median value is used as the critical temperature of the tube.

Using the bi-section algorithm, the critical temperatures of some DNTs with different radii are obtained and listed in table 2. It tells us that the values of the critical temperatures

are between 320 K and 350 K. It is interesting that the critical temperature is higher for a DNT with lower radius. Intuitively, at the same temperature, a DNT with higher curvature should be weaker due to larger pre-stretched strain of its sp^2-sp^3 bonds in the outer layer. But in the double-layered nanotube, the potential energy of the system depends not only on the strain energy but also on the non-bonding interaction-induced energy. It is known that the bond lengths of the sp^2-sp^3 in a diamondene should be between 0.14 and 0.16 nm [26], and the sp^3-sp^3 bonds are longer than 0.16 nm. The equilibrium distance between two neighbor non-bonding carbon atoms is ~ 0.34 nm. In diamondene, a central atom has three or four covalently bonded atoms. The number of neighbor atoms which provide repulsion to the central atom is no more than 12. Moreover, the repulsion is weak because the atom-atom distances are near 0.34 nm. However, the central atom is attracted by a large number of neighboring atoms with a distance between 0.34 and 1.02 nm (the cutoff of the Lennard-Jones potential [37]). The number of neighboring atoms is higher for a central atom in a DNT with lower radius.

Table 1. Tests of the thermal stability of DNTs with different initial radii at finite temperatures.

(a) Armchair DNT ((m, m)) with axial length of ~2.26 nm																			
T/K	14	16	18	20	22	24	26	28	30	32	34	36	38	40	42	44	46	48	
Radius/Å	9.69	11.08	12.46	13.85	15.23	16.62	18.00	19.39	20.77	22.15	23.54	24.92	26.31	27.69	29.08	30.46	31.85	33.23	
1 K	S	S	S	S	S	S	S	S	S	S	S	S	S	S	S	S	S	S	S
100 K	S	S	S	S	S	S	S	S	S	S	S	S	S	S	S	S	S	S	S
200 K	S	S	S	S	S	S	S	S	S	S	S	S	S	S	S	S	S	S	S
300 K	S	S	S	S	S	S	S	S	S	S	S	S	S	S	S	S	S	S	S
350 K	S	S	I	I	I	I	I	I	I	I	I	I	I	I	I	I	I	I	I
400 K	I	I	I	I	I	I	I	I	I	I	I	I	I	I	I	I	I	I	I
450 K	I	I	I	I	I	I	I	I	I	I	I	I	I	I	I	I	I	I	I
600 K	I	I	I	I	I	I	I	I	I	I	I	I	I	I	I	I	I	I	I
900 K	NT	NT	I	I	I	I	I	I	I	I	I	I	I	I	I	I	I	I	I

(b) Zigzag DNTs ((n, 0)) with axial length of ~2.61 nm																			
T/K	19	20	21	25	27	31	33	35	39	43	47	51	53	55	57	59	61	63	
Radius/Å	8.39	8.79	9.19	9.99	10.79	12.39	13.19	13.99	15.59	17.19	18.79	20.38	21.18	21.98	22.78	23.58	24.38	25.18	
1 K	S	S	S	S	S	S	S	S	S	S	S	S	S	S	S	S	S	S	S
100 K	S	S	S	S	S	S	S	S	S	S	S	S	S	S	S	S	S	S	S
200 K	S	S	S	S	S	S	S	S	S	S	S	S	S	S	S	S	S	S	S
300 K	S	S	S	S	S	S	S	S	S	S	S	S	S	S	S	S	S	S	S
350 K	NT	S	S	S	S	S	I	I	I	I	I	I	I	I	I	I	I	I	I
400 K	NT	NT	NT	I	I	I	I	I	I	I	I	I	I	I	I	I	I	I	I
450 K	NT	NT	NT	I	I	I	I	I	I	I	I	I	I	I	I	I	I	I	I
600 K	NT	NT	NT	I	I	I	I	I	I	I	I	I	I	I	I	I	I	I	I
900 K	NT	NT	NT	NT	NT	I	I	I	I	I	I	I	I	I	I	I	I	I	I

Table 2. Critical temperatures of DNTs in stable state.

A-DNT	Radius/Å	T_{Cr}/K	Z-DNT	Radius/Å	T_{Cr}/K
((18, 18))	12.46	345	((35, 0))	13.99	336
((22, 22))	15.23	340	((39, 0))	15.59	342
((26, 26))	18.00	336	((43, 0))	17.19	330
((30, 30))	20.77	323	((47, 0))	18.79	326
((34, 34))	23.54	326	((51, 0))	20.38	326
((38, 38))	26.31	328	((55, 0))	21.98	323
((42, 42))	29.08	322	((59, 0))	23.58	323
((46, 46))	31.85	325	((63, 0))	25.18	324

It means that the slimmer DNT has stronger self-attraction which leads to shrinkage of the tube. In shrinkage, the sp^2-sp^3 bonds in the outer layer have lower strains than their initial strains. This is the essential reason that the slimmer DNT is unstable at higher temperature.

3.3. Configurations of a DNT in an 'NT' state during relaxation

In table 1, a couple of DNTs, e.g. ((19, 0)) at 400 K, are in an 'NT' state after relaxation. The snapshots in figure 3 suggest that the slim DNT starts to deform seriously after only 2 ps of relaxation. At 3 ps, the upper-right part of the tube breaks, which can be verified by the local bond topology in the red circle. At 7 ps, the oval-shaped cross section has two break areas (in red circles). After 500 ps of relaxation, the tube is heavily damaged.

Two major factors result in such state of the DNT. One is the large curvature due to small radius of the tube. Each longitudinal section of the tube is under a bent state with the stretched outer surface and compressed inner surface. A lower

radius of tube means stronger stretch and compression on both surfaces. Hence, the sp^2-sp^3 bonds in the outer layer of the slim tube are easily broken. It is also found that the initial breakage appears randomly due to random distribution of the velocities of the atoms in the tube in a thermostat. This is relevant to the second essential factor, i.e., the temperature of the system. At a higher temperature, the amplitude of the thermal vibration of an atom is stronger. The bond between two atoms, e.g., the i th and j th atoms, is broken when their distance is over 0.2 nm according to the AIREBO potential. Therefore, $r_{ij} + a_T < 0.2$ nm should be satisfied if the bond is stable, where r_{ij} is the bond length, and a_T is the amplitude of thermal vibration of the bond. Thus, a higher temperature means lower stability for a given bond. This is the reason for the Z-DNT ((19, 0)) being stable at 300 K but unstable at 400 K. Similarly, at the same temperature, a larger radius of the tube means greater stability. For example, at 350 K, ((19, 0)) is unstable, but ((20, 0)) is stable.

3.4. Distribution of bond breaking in DNTs

As aforementioned, some DNTs have bond breaking during relaxation. Statistics of the bond breaking of some DNTs at room temperature or at higher temperature are listed in table 3. For DNTs at 300 K, they have a few broken bonds in the interlayer. For example, the A-DNT ((30, 30)) has two broken bonds, and the Z-DNT ((57, 0)) has four broken bonds in the interlayer. Both the outer and the inner layers of the DNTs remain undamaged.

At 900 K, the number of broken bonds exceeds half of the total amount in the interlayer of a DNT. For example, 376 of total 540 interlayer bonds in DNT ((30, 30)) break. The

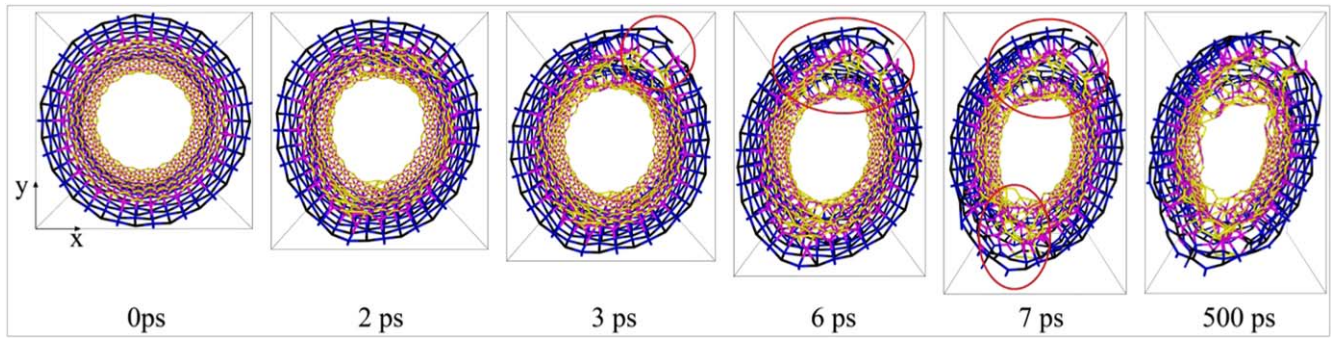


Figure 3. Perspective view of representative snapshots of a Z-DNT ((19, 0)) during relaxation at 400 K. Serious breakage is circled in red.

Table 3. Number of the sp^2 - sp^3 bonds in DNTs with different initial radius after relaxation at 300 K and 900 K. Labels ‘Inter’, ‘Inner’ and ‘Outer’ represent the bond numbers in the interlayer, inner layer, and outer layer of a DNT, respectively. Symbol ‘A-b’, e.g., 540–376, equals the initial number (in gray) subtracting the number of broken bonds (in black). The cutoff of the bond length is 2 Å.

T	300 K					900 K				
	Chirality	Radius/Å	Inter	Inner	Outer	Chirality	Radius/Å	Inter	Inner	Outer
A-DNT	((22,22))	15.23	396-0	1188-0	1188-0	((30,30))	20.77	540-376	1620-0	1620-0
	((26,26))	18.00	468-1	1404-0	1404-0	((34,34))	23.54	612-430	1836-0	1836-0
	((30,30))	20.77	540-2	1620-0	1620-0	((38,38))	26.31	684-477	2052-0	2052-0
	((34,34))	23.54	612-2	1836-0	1836-0	((42,42))	29.08	756-547	2268-0	2268-0
	((38,38))	26.31	684-3	2052-0	2052-0	((46,46))	31.85	828-593	2484-0	2484-0
Z-DNT	((35,0))	13.99	420-1	1260-0	1260-0	((39,0))	15.59	468-317	1404-0	1404-0
	((39,0))	15.59	468-2	1404-0	1404-0	((47,0))	18.79	564-388	1692-0	1692-0
	((47,0))	18.79	564-2	1692-0	1692-0	((55,0))	21.98	660-463	1980-0	1980-0
	((55,0))	21.98	660-3	1980-0	1980-0	((59,0))	23.58	708-501	2124-0	2124-0
	((57,0))	22.78	684-4	2052-0	2052-0	((63,0))	25.18	756-537	2268-1	2268-2

ratio of broken bonds to the total bonds is $\sim 70\%$. Except Z-DNT ((63, 0)), any one of the rest of the DNTs in table 3 has no bond breaking in either the outer or the inner layer. Hence, we conclude that the interlayer bonds in a DNT are weaker than those in the outer layer, and the bonds in the inner layer are the most stable.

From the number of broken bonds in the DNTs listed in table 3, we know that the number of broken bonds in the interlayer changes from less than 10 at 300 K to $\sim 70\%$ of the total amount at 900 K. The variation of bond breaking in the interlayer between 300 K and 900 K is given in figure 4, which indicates the number of broken bonds rapidly increases with temperature. At 600 K, over half of the interlayer bonds break after relaxation. But at temperatures < 300 K, there is no broken bond in the interlayer, which indicates that the tubes are stable. When the temperature is not lower than 400 K, the broken ratio depends slightly on the geometry of the DNT. One can also find that at the same temperature, DNT with a higher radius has a higher value of broken ratio. For example, at 400 K, A-DNT ((26, 26)) has a broken ratio of $\sim 7.7\%$, but ((30, 30)) has a broken ratio of $\sim 12.2\%$. The reason is, as mentioned previously, that the slimmer DNT has higher self-attraction which prevents the breaking of interlayer bonds.

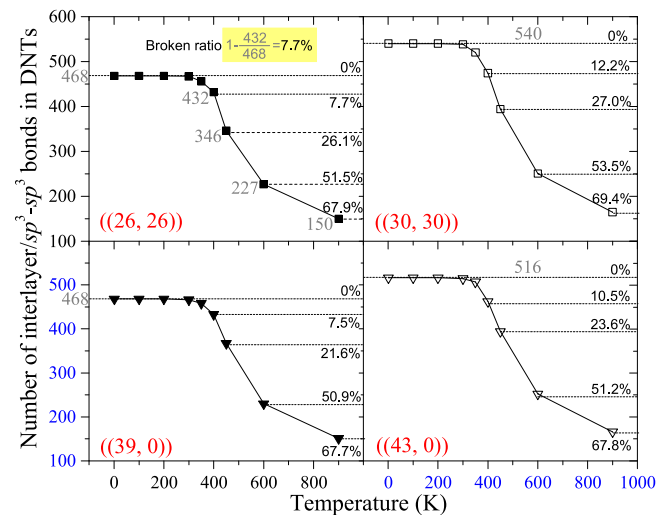


Figure 4. Number of the interlayer (sp^3 - sp^3) bonds in DNTs versus temperature.

Figure 5(a) illustrates the distributions of broken bonds in the interlayer of a DNT. Distributions of the broken bonds are not strictly uniform. For example, within a red circle, the bonds distribute sparsely due to the lack of broken bonds. For

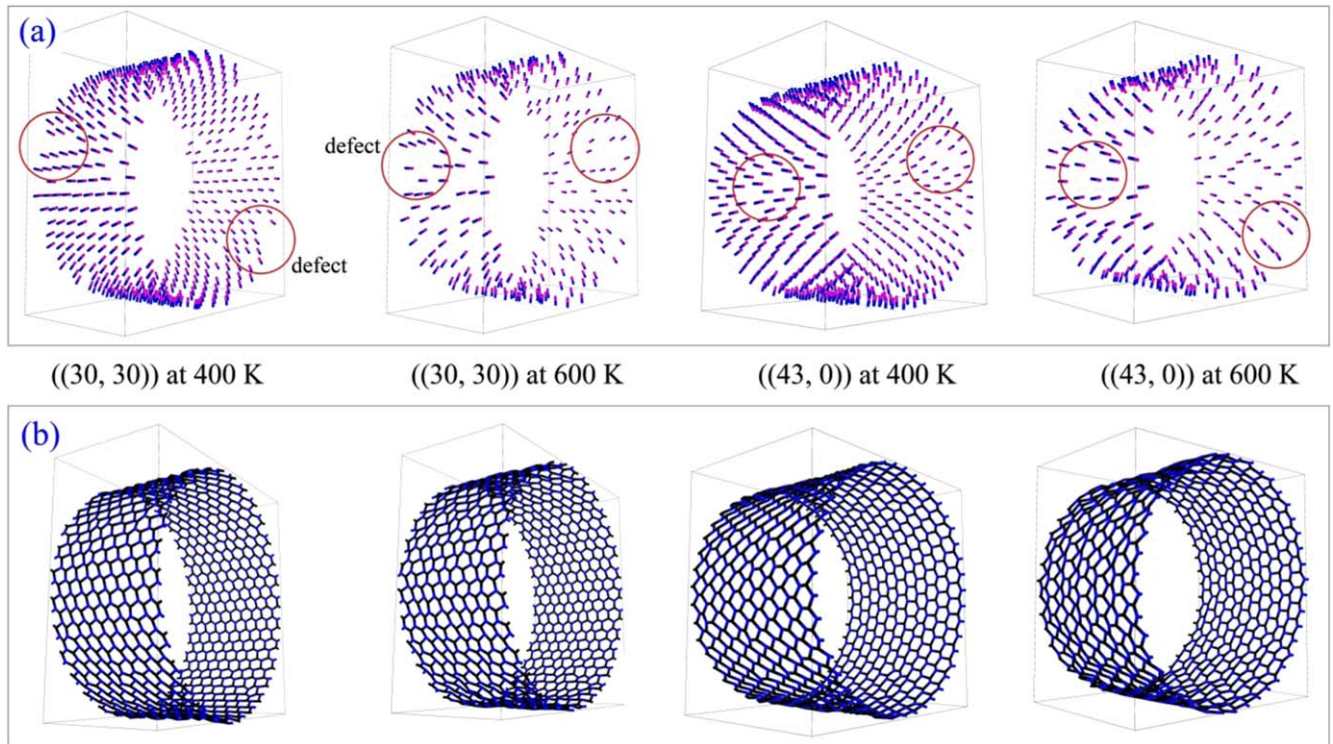


Figure 5. Distributions of broken bonds in DNTs at 400 K and 600 K. (a) Distribution of interlayer bonds. (b) Distribution of bonds in the outer layers. The cutoff of the bond length is 2 Å.

the same DNT, it has more broken bonds at higher temperature, e.g., 600 K. For comparison, we also give the layout of covalent bonds in the outer layers of four tubes. For the two DNTs, they have no bond breaking in the outer layers during relaxation at both 400 K and 600 K and the shape of its outer layer changes at different temperature. For example, the distribution of atoms is more uniform at lower temperature, which means weaker thermal vibration of the atoms.

3.5. Bond lengths and bond angles in DNTs

Here, we choose two representative cells at different locations in a DNT to calculate the bond lengths and bond angles at finite temperatures. For example, at location A in the initial configuration of a DNT ((30, 30)), $\theta_1 = -143.9^\circ$, and $z_1 = 1.067$ nm. At location B, $\theta_1 = 120.0^\circ$, and $z_1 = 1.067$ nm. In the initial configuration of a DNT ((43, 0)), $\theta_1 = -121.4^\circ$, and $z_1 = 1.192$ nm at location A; $\theta_1 = 138.1^\circ$, and $z_1 = 1.192$ nm at location B. The mean values between 401 and 500 ps are obtained to draw the curves in figure 6.

At temperatures below 400 K, the bond lengths and bond angles vary slightly. This means that the sizes of the bond angles and bond lengths depend weakly on temperature. At 400 K, either at location A or B in a DNT, bond 2–3 or bond 6–7 may break (i.e., L_{23} or $L_{67} > 0.2$ nm). From figure 1(a), we know that the two bonds are sp^3 – sp^3 bonds, i.e., interlayer bonds. At location B in the A-DNT ((30, 30)), the two bonds are in the same longitudinal section. Breakage of bond 2–3 accompanies a bond length decrease of the other neighbor bonds (the lower layer in figure 6(a)). For example, bond 3–5, which is ~ 0.155 nm at temperature < 400 K, shrinks to

~ 0.141 nm, and bond 0–2 shrinks from ~ 0.148 to ~ 0.137 nm. The reason is the local relaxation after breakage of bond 2–3. During local relaxation, both neighbor bond lengths (figure 6(a)) and bond angles have obvious changes (figure 6(b)). For instance, bond angle α_{135} exceeds 120° . At 600 K or 900 K, bond 2–3 at both locations breaks. Especially bond 6–7 breaks synchronously at 900 K. Meanwhile, the rest of the bonds remain stable. This matches the results in table 3 very well, i.e., most of the interlayer bonds break but there is no bond breakage in either the outer layer or the inner layer of the tube.

In the Z-DNT ((43, 0)), bonds 2–3 and 6–7 are in the same cross section of the tube. Hence, when one of them breaks, the other does not change. But their neighbor bond lengths and bond angles change obviously. For example, at location B, bond 2–3 breaks at 550 K. At the same time, bond 6–7 changes slightly, but bonds 0–2, 1–3, 2–4, and 3–5 shrink obviously. Meanwhile, bond angle α_{357} becomes higher than 120° .

3.6. Thermal behavior of the cross section of DNTs

To reveal the thermal deformation of the cross section of a DNT, we calculate the diameters of the inner and the outer layers of a tube at finite temperatures using equations (1) and (2). The bond lengths, bond angles, and the chirality factor m or n in the equations need to be obtained before calculation. For example, to calculate the diameter of the inner layer of the A-DNT ((30, 30)) at 100 K, bond lengths L_{02} and L_{24} should be obtained and bond angle α_{024} is needed plus $m = 30$. To obtain the bond angles and bond lengths, we choose two

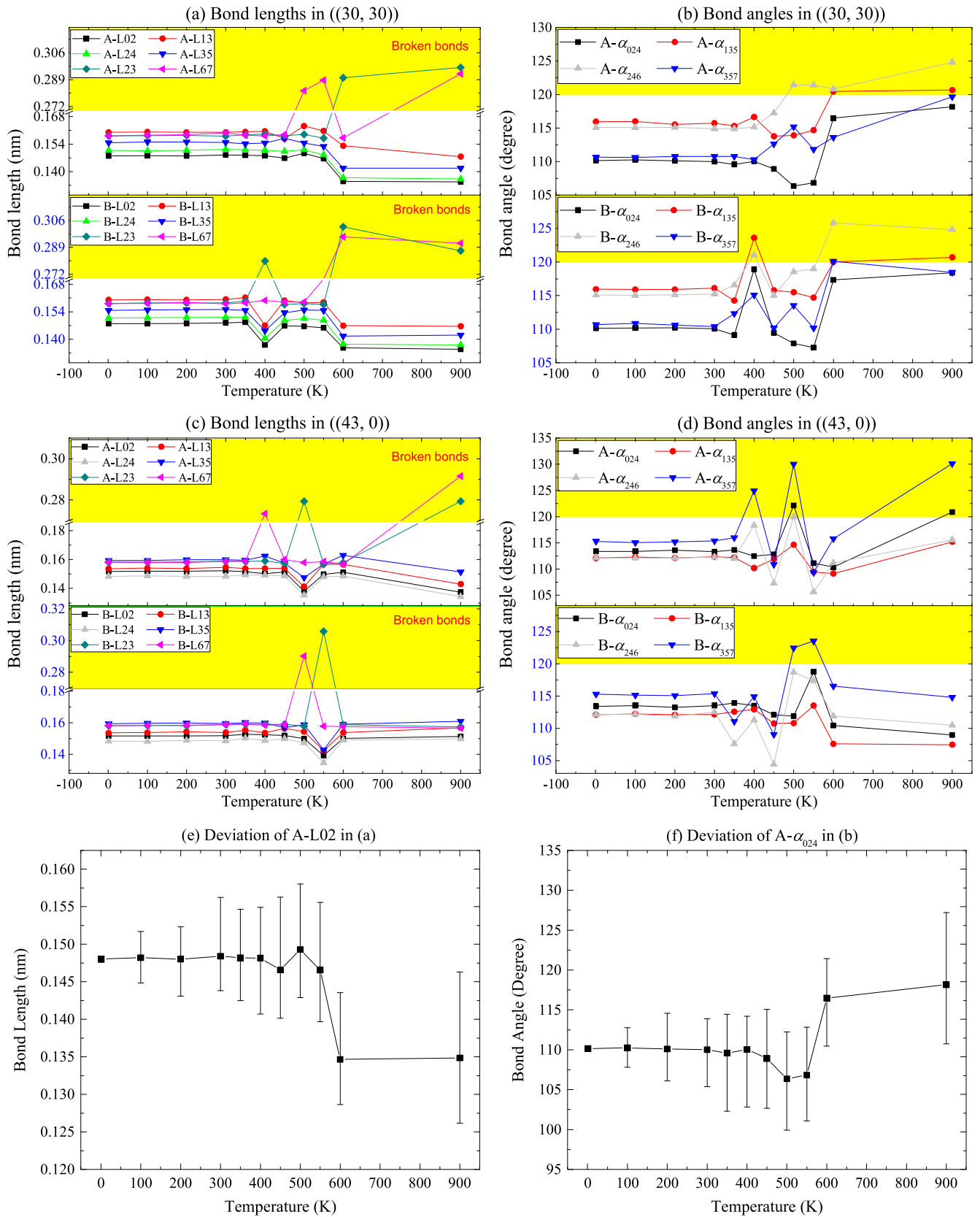


Figure 6. Bond lengths and bond angles in DNTs at finite temperature. (e) and (f) show the typical deviation of representative bond length A-L02 in (a) and bond angle A- α_{024} in (b).

Table 4. Mean diameters of DNTs at finite temperatures obtained by time averaging between 401 and 500 ps during relaxation (unit: nm).

T	A-DNT ((30, 30))						Z-DNT ((43, 0))					
	Inner layer			Outer layer			Inner layer			Outer layer		
	A	B	Mean	A	B	Mean	A	B	Mean	A	B	Mean
1 K	1.9096	1.9093	1.9094	2.1745	2.1747	2.1746	1.6847	1.6846	1.6847	1.8426	1.8426	1.8426
100 K	1.9130	1.9105	1.9117	2.1788	2.1757	2.1772	1.6865	1.6858	1.6862	1.8418	1.8448	1.8433
200 K	1.9085	1.9123	1.9104	2.1661	2.1749	2.1705	1.6861	1.6881	1.6871	1.8448	1.8444	1.8446
300 K	1.9113	1.9121	1.9117	2.1692	2.1821	2.1757	1.6914	1.6915	1.6915	1.8478	1.8483	1.8481
350 K	1.8984	1.8930	1.8957	2.1597	2.1460	2.1529	1.6900	1.6590	1.6745	1.8518	1.8021	1.8270
400 K	1.9078	1.9566	1.9322	2.1947	2.1662	2.1804	1.6872	1.6785	1.6829	1.8708	1.8371	1.8540
450 K	1.8643	1.8777	1.8710	2.1011	2.1623	2.1317	1.6466	1.6148	1.6307	1.8040	1.7396	1.7718
500 K	1.8315	1.8406	1.8361	2.1562	2.1491	2.1527	1.6774	1.6689	1.6732	1.9343	1.8106	1.8725
550 K	1.8095	1.8156	1.8126	2.1434	2.1328	2.1381	1.6190	1.6535	1.6363	1.7700	1.8378	1.8039
600 K	1.8680	1.8973	1.8826	2.1472	2.0780	2.1126	1.6795	1.6870	1.6833	1.8816	1.8588	1.8702
900 K	1.9001	1.9088	1.9044	2.0977	2.0909	2.0943	1.5600	1.6864	1.6232	1.8618	1.8556	1.8587

different locations in the tube after full relaxation at a specified temperature. The diameter is evaluated at both locations, and the median is used as the diameter of the layer. For example, the diameter of the inner layer is ~ 1.9130 nm at location A, and ~ 1.9105 nm at location B. Their median is 1.9117. Using the same method, we obtain the results listed in table 4.

For the A-DNT ((30, 30)) at 1 K, the mean diameter is ~ 1.9094 nm for the inner layer, and ~ 2.1746 nm for the outer layer. The two values can be considered as the original sizes of the cross section. At 100 K, the two diameters grow to be ~ 1.9117 nm and ~ 2.1772 nm, respectively. This means that the cross section has thermal expansion between 1 K and 100 K. From the results in table 4, without considering breaking bonds, there is no thermal expansion for the DNT at temperature between 100 K and 300 K. At 400 K, the two values of the diameter evaluated at both locations are obviously different. The reason is that the bond 2–3 breaks at location B, but remains stable at location A. With the exception of the results at 400 K, the values of the diameters of the two layers at temperatures between 450 K and 600 K are less than those at 1 K, respectively, which implies that the tube's cross section shrinks at such high temperatures. Similarly, the Z-DNT ((43, 0)) also has shrinkage of the cross section at 350 K, 450 K, or 550 K.

If we consider the broken ratio of the interlayer bonds in the tubes, the situation may be different. Figure 6(a) illustrates that the A-DNT ((30, 30)) is stable at both locations when the temperature is 350 K or 450 K. At 350 K, the mean values of the diameters of the tube are ~ 1.8957 nm of the inner layer and ~ 2.1529 nm of the outer layer. Both values are less than those at 1 K, respectively. At 450 K, the diameters are ~ 1.8710 nm and ~ 2.1317 nm, and are less than those at 350 K, respectively. Hence, we conclude that the perfect A-DNT has thermal shrinkage at relatively higher temperatures.

Figure 6(c) shows that the Z-DNT ((43, 0)) is stable at both locations when the temperature is 350 K or 600 K, respectively. At 350 K, the two diameters of both layers are 1.6745 nm (< 1.6847 nm at 1 K) and 1.8270 nm (< 1.8426 nm at 1 K). At 600 K, the two diameters are 1.6833 nm (< 1.6847 nm at 1 K) and 1.8702 nm (> 1.8426 nm at 1 K). From the broken ratio given in figure 4 we know that the tube has been heavily damaged at 600 K. Coincidentally, at locations A and B, the interlayer bonds are stable. Hence, we find that the diameters calculated by equations (1) and (2) are not reliable at such high temperatures. The values of the diameters of the tubes with a very low broken ratio of the interlayer bonds are acceptable to show the thermal property of the tube, i.e., the cross section has thermal expansion between 1 K and 100 K but no thermal expansion between 100 K and 300 K.

3.7. Thermal behavior of the tube axis of DNTs

Along the tube axis, the thermal behavior of an A-DNT ((30, 30)) is also demonstrated. In this case, we choose four tubes with different initial lengths, i.e., 2.26, 4.52, 6.03, and 7.53 nm, to discuss the length effect on the thermal property. Meanwhile, three temperatures are involved in simulations to show the temperature effect. We choose 1 K as a standard for comparison among the final tube lengths after relaxation. As mentioned above, the DNT is stable at 300 K but not at 500 K. The two temperatures are chosen to show the dependency of the thermal property on the broken ratio of the interlayer bonds. The relaxation histories of the four tubes at three different temperatures are given in figure 7.

After full relaxation, the four tube lengths are 2.2907, 4.5814, 6.1085, and 7.6356 nm at 1 K. Correspondingly, they are 2.2959, 4.5926, 6.1228, and 7.6542 nm at 300 K. To show the length effect, we define the thermal strain, which equals the length difference at two temperatures divided by the initial length at 1 K. Hence, the thermal strains are 0.2270% with respect to the initial length of 2.26 nm, 0.2445% (to the initial

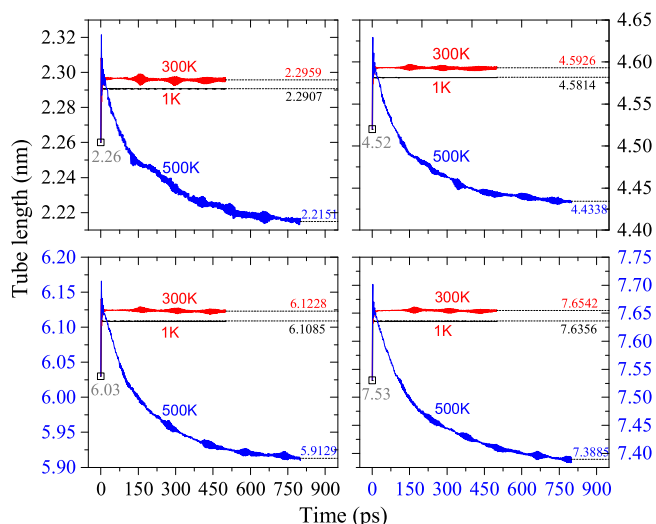


Figure 7. Shrinking process of the DNT ((30, 30)) with different initial lengths during relaxation. The initial tube lengths are 2.26, 4.52, 6.03, and 7.53 nm before relaxation.

length of 4.52 nm), 0.2341% (to the initial length of 6.03 nm), and 0.2436% (to the initial length of 7.53 nm). The highest relative difference is 7.7% among the four cases. Hence, the initial tube length has a slight influence on the thermal expansion of the tube. It also shows that the stable DNT has thermal expansion between 1 K and 300 K.

When relaxing the tubes at 500 K, the final tube lengths are 2.2151, 4.4338, 5.9129, and 7.3885 nm. The corresponding thermal strains are -3.3003% , -3.2217% , -3.2021% , and -3.2362% when compared to the lengths at 1 K. The results also indicate that the initial tube length has a slight effect on the thermal behavior of the tube. Negative values demonstrate that the DNT has thermal shrinkage. At 500 K, the interlayer bonds of the tube break heavily. From figure 4, we estimate that the broken ratio of the interlayer bonds in the tube should be between 27.0% and 53.5%. Figure 5(a) further indicates that the broken bonds distribute relatively uniformly (see the bond layout in the ((30, 30)) at 600 K). Hence, we conclude that the broken DNT has shrinkage along the tube axis. The reason is that the bond angle α_{235} reduces when bond 2–3 is broken. Meanwhile, the neighbor bonds shrink during local relaxation. Hence, local bond configurations change greatly, which can be verified by the irregular honeycomb in the outer layer of the tube (figure 5(b)).

4. Conclusions

A DNT can be formed by curving a rectangular diamondene followed with sewing the two straight edges. Thermal stabilities of DNTs are investigated using molecular dynamics simulation approaches. Some conclusions and phenomena are demonstrated, as discussed below.

Firstly, the potential energy per atom is higher in the DNT with smaller radius. At 1 K, the values of the VPE per atom drop monotonously with the increase of the radii of

DNTs and are independent of the chirality of the DNTs with similar radii. Due to breaking interlayer bonds, the values of the VPE per atom at 900 K are one order of magnitude larger than those at 1 K.

Secondly, the interlayer bonds, i.e., the sp^3 – sp^3 bonds, in the DNTs are not stable when the temperature is higher than 300 K. When the temperature is not lower than 400 K, the broken ratio depends slightly on the geometry of the DNT. The broken bonds distribute approximately uniformly. A few sp^2 – sp^3 bonds in the outer or inner layer break.

Thirdly, DNTs have critical temperatures between 320 K and 350 K. The critical temperature is higher for a DNT with lower radius due to stronger self-attraction of the atoms in the tube.

Finally, for a stable DNT, it has thermal expansion when heated. For an unstable DNT with a high broken ratio of interlayer bonds, it has thermal shrinkage in both the cross section and the tube length. The reason is that the local relaxation at the broken interlayer bonds leads to an obvious change in the neighboring bond lengths and bond angles.

The conclusions provide guidelines for storing stable DNTs. For the damaged DNTs, their thermal shrinkage is significant for the design and fabrication of metamaterials.

Acknowledgments

The authors state that there is no competing financial interest. This work is financially supported by the National Natural Science Foundation, China (Grant No. 11472098), and the National Key Research and Development Plan, China (Grant No. 2017YFC0405102).

ORCID iDs

Lei Wang <https://orcid.org/0000-0002-2770-5022>

Yi Min Xie <https://orcid.org/0000-0001-5720-6649>

Qing-Hua Qin <https://orcid.org/0000-0003-0948-784X>

References

- [1] Kroto H W, Heath J R, O'Brien S C, Curl R F and Smalley R E 1985 C60: Buckminsterfullerene *Nature* **318** 162–3
- [2] Iijima S 1991 Helical microtubules of graphitic carbon *Nature* **354** 56–8
- [3] Lima M D *et al* 2012 Electrically, chemically, and photonically powered torsional and tensile actuation of hybrid carbon nanotube yarn muscles *Science* **338** 928–32
- [4] Kim S H *et al* 2017 Harvesting electrical energy from carbon nanotube yarn twist *Science* **357** 773–8
- [5] Novoselov K S, Geim A K, Morozov S V, Jiang D, Zhang Y, Dubonos S V, Grigorieva I V and Firsov A A 2004 Electric field effect in atomically thin carbon films *Science* **306** 666–9
- [6] Lee C, Wei X, Kysar J W and Hone J 2008 Measurement of the elastic properties and intrinsic strength of monolayer graphene *Science* **321** 385–8
- [7] Cao Y, Fatemi V, Fang S, Watanabe K, Taniguchi T, Kaxiras E and Jarillo-Herrero P 2018 Unconventional

- superconductivity in magic-angle graphene superlattices *Nature* **556** 43–50
- [8] Frondel C and Marvin U B 1967 Lonsdaleite, a hexagonal polymorph of diamond *Nature* **214** 587–9
- [9] Zheng Q and Jiang Q 2002 Multiwalled carbon nanotubes as gigahertz oscillators *Phys. Rev. Lett.* **88** 045503
- [10] Legoas S B, Coluci V R, Braga S F, Coura P Z, Dantas S O and Galvao D S 2003 Molecular dynamics simulations of carbon nanotubes as gigahertz oscillators *Phys. Rev. Lett.* **90** 055504
- [11] Guo W, Guo Y, Gao H, Zheng Q and Zhong W 2003 Energy dissipation in gigahertz oscillators from multiwalled carbon nanotubes *Phys. Rev. Lett.* **91** 125501
- [12] Cai K, Yin H, Qin Q H and Li Y 2014 Self-excited oscillation of rotating double-walled carbon nanotubes *Nano Lett.* **14** 2558–62
- [13] Fennimore A, Yuzvinsky T, Han W Q, Fuhrer M, Cumings J and Zettl A 2003 Rotational actuators based on carbon nanotubes *Nature* **424** 408–10
- [14] Barreiro A, Rurali R, Hernández E R, Moser J, Pichler T, Forró L and Bachtold A 2008 Subnanometer motion of cargoes driven by thermal gradients along carbon nanotubes *Science* **320** 775–8
- [15] Wang B, Vuković L and Král P 2008 Nanoscale rotary motors driven by electron tunneling *Phys. Rev. Lett.* **101** 186808
- [16] Cai K, Li Y, Qin Q H and Yin H 2014 Gradientless temperature-driven rotating motor from a double-walled carbon nanotube *Nanotechnology* **25** 505701
- [17] Aust R B and Drickamer H G 1963 Carbon: a new crystalline phase *Science* **140** 817–9
- [18] Chernozatonskii L A, Sorokin P B, Kvashnin A G and Kvashnin D G 2009 Diamond-like C₂H nanolayer, daimane: simulation of the structure and properties *JETP Lett.* **90** 134–8
- [19] Chernozatonskii L A, Sorokin P B, Kuzubov A A, Sorokin B P, Kvashnin A G, Kvashnin D G, Avramov P V and Yakobson B I 2011 Influence of size effect on the electric and elastic properties of diamond films with nanometer thickness *J. Phys. Chem. C* **115** 132–6
- [20] Utsumi W and Yagi T 1991 Light-transparent phase formed by room-temperature compression of graphite *Science* **252** 1542–4
- [21] Mao W L, Mao H K, Eng P J, Trainor T P, Newville M, Kao C C, Heinz D, Shu J F, Meng Y and Hemley R J 2003 Bonding changes in compressed superhard graphite *Science* **302** 425–7
- [22] Barboza A P M, Guimaraes M H D, Massote D V P, Campos L C, Barbosa Neto N M, Cancado L G, Lacerda R G, Chacham H, Mazzoni M S C and Neves B R A 2011 Room-temperature compression-induced diamondization of few-layer graphene *Adv. Mater.* **23** 3014–7
- [23] Odkhuu D, Shin D, Ruoff R S and Park N 2013 Conversion of multilayer graphene into continuous ultrathin sp³-bonded carbon films on metal surfaces *Sci. Rep.* **3** 3276
- [24] Martins L G P et al Raman evidence for pressure-induced formation of diamondene *Nat. Commun.* 2017 **8** 96
- [25] Gao Y, Cao T F, Cellini F, Berger C, de Heer W A, Tosatti E, Riedo E and Bongiorno A 2018 Ultrahard carbon film from epitaxial two-layer graphene *Nat. Nanotechnol.* **13** 133–8
- [26] Shi J, Cai K and Xie Y M 2018 Thermal and tensile properties of diamondene at finite temperature: a molecular dynamics study *Mater. Des.* **156** 125–34
- [27] Cai K, Wang L and Xie Y M 2018 Buckling behavior of nanotubes from diamondene *Mater. Des.* **149** 34–42
- [28] Wang L, Cai K, Wei S and Xie Y M 2018 Softening-to-hardening of stretched diamondene nanotubes *Phys. Chem. Chem. Phys.* **20** 21136–43
- [29] LAMMPS, Molecular Dynamics Simulator. (<http://lammps.sandia.gov/>) (Retrieved May 18, 2018)
- [30] Cai K, Cai H F, Yin H and Qin Q H 2015 Dynamic behavior of curved double-wall carbon nanotubes with rotating inner tube *RSC Adv.* **5** 29908–13
- [31] Nosé S 1984 A unified formulation of the constant temperature molecular dynamics methods *J. Chem. Phys.* **81** 511–9
- [32] Hoover W 1985 Canonical dynamics: equilibrium phase-space distributions *Phys. Rev. A* **31** 1695–7
- [33] Stuart S J, Tutein A B and Harrison J A 2000 A reactive potential for hydrocarbons with intermolecular interactions *J. Chem. Phys.* **112** 6472–86
- [34] Li S Z, Li Q Y, Carpick R W, Gumbsch P, Liu X Z, Ding X D, Sun J and Li J 2016 The evolving quality of frictional contact with graphene *Nature* **539** 541–6
- [35] Cai K, Yu J Z, Wan J, Yin H, Shi J and Qin Q H 2016 Configuration jumps of rotor in a nanomotor from carbon nanostructures *Carbon* **101** 168–76
- [36] Yang L K, Cai K, Shi J and Qin Q H 2017 Significance tests on the output power of a thermally driven rotary nanomotor *Nanotechnology* **28** 215705
- [37] Jones J E 1924 On the determination of molecular fields: II. From the equation of state of a gas *Proc. R. Soc. London* **106** 463–77